

Full-length article

Systematic analysis of the flow field within low-swirl combustors

Paolo Gobbato^{a,*}, Massimo Masi^b, Alessandro Cappelletti^c, and Marco Antonello^b

^a University of Padova, Department of Industrial Engineering, Via Venezia, 1 - 35131, Padova, Italy

^b University of Padova, Department of Management and Engineering, Stradella S. Nicola, 3 - 36100, Vicenza, Italy

^c University of Florence, Department of Industrial Engineering, Via di S. Marta, 3 - 50139, Florence, Italy

Abstract

Swirling flows through sudden expansions is a common solution adopted to stabilise the flame within combustion systems. Fuel-air mixing promoted by the swirling motion contributes also to complete the fuel oxidation and reduce pollutant emissions.

Most of the experimental studies appeared in the literature investigated the aerodynamics of high-swirl combustors. In such combustors the expansion of the flow in the combustion chamber produces a central recirculation zone (CRZ) which provides a stable anchoring to the flame. By comparison, few studies analyse the structure of the flow field with weak swirl, although the capability of low-swirl combustors to generate stable flames over a wide range of thermal loads was experimentally demonstrated.

This study deals with low-swirling flows generated by axial swirlers and aims at providing a comprehensive insight of the flow field by considering the effect of some relevant parameters not yet systematically investigated. Data taken from the literature of axial and tangential velocities measured on combustors of similar geometry and swirl number are compared in order to evaluate the effect of the Reynolds number and the main design parameters on the flow field. The literature database is

* Corresponding author.

E-mail address: paolo.gobbato@unipd.it

Phone: +39 049 827 6748

extended considering original measurements performed by the authors on a laboratory combustor. The comparison shows that the flow field of low-swirl combustors is mainly affected by the Reynolds number. Among the design parameters considered, the expansion ratio is the most significant. In particular, the former controls the radial position of the velocity peak whereas the latter influences the axial decay of velocity within the jet core.

Keywords: low-swirl combustor, isothermal swirling flow, hot-wire velocity measurement.

1. Introduction

Swirling flows are frequently used to increase the performance of industrial combustors operating with high volumetric heat-release rates. They are generated by inserting a row of guide vanes (known as a swirler) within the burner or providing tangential inlets into the burner or the combustion chamber (swirl generators) [1]. Rotating vanes, grids, or tubes have sometimes been applied for experimental investigations of swirling jets, as well [2].

Swirling flow combustors may operate both with non-premixed and premixed flames. In non-premixed flames, combustion is controlled by mixing, meaning that the flame occurs only in the zones where the reactants generate a flammable mixture. From this point of view non-premixed flames do not propagate. On the other hand, a premixed flame can be properly considered as a combustion wave propagating through a flammable mixture at subsonic speed. Therefore, the premixed flame speed is kinetically controlled, i.e. it is controlled by mixture composition, thermodynamic state of reactants, and turbulence intensity [3]. This different nature of flames has a significant impact on the operation of swirling flow combustors. In non-premixed combustors, swirling motion is essentially used to promote mixing between fuel and air in order to increase the combustion intensity and complete fuel oxidation. Although mixing is also essential in premixed combustors in order to sustain the flame, swirling flows in premixed combustors are used to locally

reduce the axial velocity of the reacting mixture and, consequently, provide a stable flame anchoring zone. The reduction of flow axial velocity is promoted also by the increase the cross-flow section which induces the swirling flow to expand. For this reason, swirling-flow burners are frequently coupled to combustion chambers of higher radial extension.

Swirl strength has a notable impact on the flow field. In high-swirl combustors, the swirling motion generates a low-pressure zone in the central core of the rotating flow. This results in a positive axial pressure gradient so that the flow reverses its direction and a toroidal recirculation (known as central recirculation zone, CRZ) is established. This recirculation zone (a kind of vortex breakdown) provides a stable source of heat for continuous ignition of the reactants exiting the burner. The shape, the extension, and the strength of the CRZ are mainly controlled by the burner geometry, although the expansion ratio and the side-wall angle have an influence, as well. An extensive review of high-swirling reacting flows and their application within combustion systems was performed by Syred and Beer [4] and Syred [5]. An early state-of-the-art of the experimental findings on swirling reacting flows and their modelling is provided in [6]. In [7] the authors analyse the types of vortex breakdown (which precedes the CRZ formation) and present the effect of inlet conditions and geometry on the structures of recirculation zones.

Most industrial premixed combustors operate with high-swirling flows because the strong and stable recirculation zone significantly reduces the risk of flame flashback and blow-off also in very lean conditions. However, high-swirling flames are prone to thermo-acoustic instabilities because the vortex breakdown may excite the acoustic field and/or couple to one of the combustor acoustic modes [2,3,5].

In low-swirl combustors, the flame stabilisation relies only on a reduction of axial velocity because the intensity of the swirling motion is not sufficient to induce the flow to recirculate along the combustor axis. Flames with low swirl have been traditionally considered as weakly stable,

although a certain swirl motion may be useful in some particular applications for increasing the flame length [1]. Quite recently, Cheng [3] proposed and tested low-swirl combustors able to generate stable flames over a wide range of thermal loads. In such combustors, the burner features an annular swirler and a central perforated plate. The resulting flow field is relatively uniform and free from the large shear stresses (characteristic of high-swirling flows) that make the flame more vulnerable to non-uniform heat release and to local quenching in ultra-lean conditions. Cheng's combustor design has been successfully applied to boilers, furnaces and gas turbines up to about 2 MW [8].

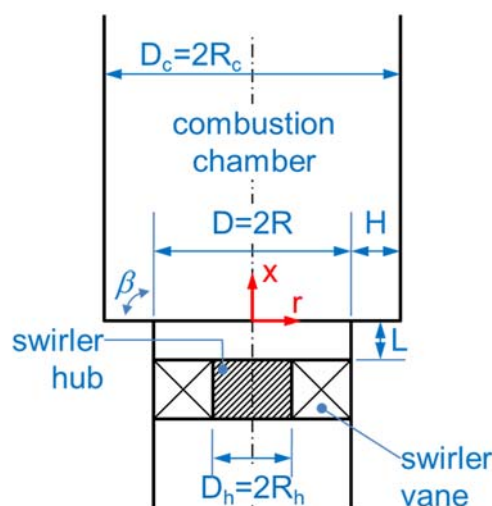


Figure 1 - Schematic of a combustor with sudden expansion including an axial swirler with guide vanes.

This study deals with low-swirling flows within small sudden-expansion combustors and aims at analysing the effect of main design and operating parameters on the mean velocity field. The analysis is performed by comparing several sets of experimental data taken from the literature with one original set of measurements acquired by the present authors on a laboratory low-swirl combustor. The new set of data allows for an extension of the literature database given the particular design and operating conditions of the test rig. It is well-known that the method of swirl generation affects the flow field, as briefly recalled in the paper. Thus, the present work focuses on flow fields generated by

axial-vaned swirlers (Fig. 1). In order to restrict the number of design parameters to consider, the paper analyses only isothermal data according to the many literature studies performed in non-reacting conditions and considering that the chemical reaction affects only slightly the flow field especially in low-swirl combustors [9–11].

The paper is organised as follows. The main design and operating parameters of swirling-flow combustors are presented in Section 2. Their effect on the flow field is summarised on the basis of results from literature studies. At the end of the section the parameters considered in the present work are specified. Then, a literature review of experimental studies dealing with the low-swirl combustor flow field is provided. The test rig and results of the experimental tests performed by the present authors are presented in Section 4 e 5, respectively. Finally, the new data are compared to the literature experimental data sets in order to delineate the trend of the modifications in the flow field within low-swirl combustors against changes of the main design and operating parameters.

2. Design and operating parameters of swirling-flow combustors

Swirling flows are commonly characterised by the swirl number S . This dimensionless quantity is defined as the ratio of axial flux of tangential momentum \dot{G}_θ to axial flux of axial momentum \dot{G}_x :

$$S = \frac{\dot{G}_\theta}{R\dot{G}_x} \quad (1)$$

The swirl number can be calculated from integration of velocity and pressure profiles or by direct measurement of torque and thrust exerted on the orifice [12]. Neglecting velocity fluctuations due to turbulence, the radial velocity component and the static pressure term in \dot{G}_x [1,2], Eq. (1) is written:

$$S = \frac{\int_0^R uw\rho r^2 dr}{R\int_0^R u^2 \rho r dr} \quad (2)$$

where u and w are the axial and the azimuthal velocities, respectively, and ρ is the flow density. The

expression can be related to the swirler geometry only (Fig. 1), by assuming very thin vanes of constant chord and angle α , and a uniform axial velocity profile [1]:

$$S = \frac{2}{3} \left[\frac{1 - (R_h/R)^3}{1 - (R_h/R)^2} \right] \tan \alpha \quad (3)$$

The expression further simplifies if the swirler is hub-less:

$$S = \frac{2}{3} \tan \alpha \quad (4)$$

Equations (3) and (4) are very useful because they allow the computation of swirl number in the case of poor spatial resolution of measurements or lack of any experimental data. However, they generally overestimate the actual swirl number of the flow, as discussed in the following.

Introduction of swirl on turbulent jets causes an increase in the rate of fluid entrainment and velocity decay [1,6,13]. Axial velocity profiles are usually Gaussian-shaped for very low swirl number [14,15]. With the increase of the swirl number, axial velocity maxima are displaced from the jet axis, resulting in a double hump-shaped velocity profile [1,6]. Transition from a Gaussian to a double hump-shape is affected by the method used to generate swirl [12,16] and by the D_h/D ratio [14,15]. In particular, the presence of a swirler hub causes a small reverse-flow region in the hub wake, which may lead to a double hump-shaped velocity profile even without swirl [1,13]. Increase the distance L (swirl recess length) helps minimize the influence of the geometry of the swirl generator on the velocity profiles at the chamber inlet [17].

The point of onset of reversed flow generally is taken to occur at approximately $S = 0.6$ [1,6]. Thus, systems operating with $S < 0.6$ are usually considered low-swirl combustors. However, swirl number is not a comprehensive parameter for classifying the effect of the inlet swirl on the flow field, and the CRZ may appear also for swirl numbers different from the critical value of 0.6. For instance, divergent-exit burners (that is for $\beta < 90^\circ$, Fig. 1) reduce the critical swirl number [1,9]. Divergent nozzles show also the combined effect of increasing the radial distance of separation between peaks

of axial and tangential velocities, if the transition to a double-hump shape of profiles has already occurred [1]. The method of swirl generation may also alter the critical value at which a CRZ appears, as discussed in [16]. Lilley [6] states that recirculation zones produced by swirl generators are generally much smaller than those produced by swirl vanes. Because of the strong dependence of the flow swirl number on the combustor geometry for similar designs, a precautionary critical value of 0.4 is considered in the following for designs like that shown in Fig. 1 [18].

Swirling flows in sudden-expansion combustors are certainly affected also by the expansion ratio, ER , defined as:

$$ER = D_c / D \quad (5)$$

Although many authors highlight the importance of this parameter [13,15], most of literature studies were performed at constant ER . The effects of ER on swirling flow with $S > 0.3$ is investigated in [19,20]. In [19], the authors found that an increase of the confinement causes a reduction of the reverse mass flow in the CRZ.

The characteristic viscous length scale for swirling flows is properly represented by the Reynolds number based on the vortex-core diameter, if present [7]. However, most of the literature data refer to the Reynolds number based upon the burner diameter:

$$Re = \frac{\rho U_D D}{\mu} \quad (6)$$

where U_D is the mean axial velocity upstream of the swirler referred to the duct diameter D and μ is the dynamic viscosity of the flow. This definition of Reynolds number is general, being valid also for weak swirling flows and will be used throughout the paper. Rhode [15] verified that in the range 70000–130000 the facility he used operates in the Reynolds number-insensitive conditions from zero to high swirl number. Dellenback [21] found that mean velocities collapse to single curves from $Re = 30000$ to $Re = 100000$ for unswirled flows. In case of vortex breakdown, Syred and Beer [4] stated

that a Reynolds number of 20000 is large enough to ensure a well-developed CRZ.

In the present study the effect of ER , D_h/D ratio, the distance L , and Reynolds number on the flow field is investigated by comparing sets of measurements of the literature and a new set of experimental data. The latter provides some additional information about the spatial evolution of the low-swirl flow field as it was acquired by the present authors on a test rig operating at high Reynolds number and featuring ER greater than that usually adopted in test rigs reported in the literature. Mean velocity fields are compared for swirl numbers as similar as possible in order to attempt to remove the effect of this parameter and focus the attention on other parameters less investigated in the literature. When swirl numbers are quite different, the effect of S on the flow field is considered. In addition, all the data sets refer to axial swirlers with constant angle α along the radius in order to remove the impact of the vane design on the tangential and axial velocity profiles [16].

3. Literature review of low-swirl flow field investigations

Flows with weak swirl motion have been quite extensively analysed to also investigate the development of a CRZ with the increase of swirl intensity [6,9,12–15,21]. On the other hand, the absence of recirculation zones and relatively high shear stresses make low-swirl flow fields well suited to validation of numerical models. This is perhaps the main reason that motivates many authors to perform testing of low-swirl combustors, especially in the early works.

The studies considered in the paper for the analysis of the flow field within low-swirl combustors with sudden expansion are summarised in the following. They represent the most relevant works found in the literature dealing with low-swirling flows generated by axial-vaned swirlers (i.e., configurations similar to that shown in Fig. 1). Refer to [13] for a recent review of the experimental studies performed from null to high swirl numbers.

A near complete set of velocity and turbulence data at three swirl numbers (0, 0.3, and 0.5) is

presented in [14]. The swirling flow is generated by a swirler with 12 curved vanes of constant angle and velocity measurements were acquired by using laser Doppler velocimetry (LDV). The results show Gaussian shaped profiles for the axial velocity at $S = 0$ in all the measurement locations, and double hump-shaped velocity profiles at $S = 0.3$. At $S = 0.5$ a recirculation zone appears in the core of the flow (CRZ), whereas a second recirculation zone (outer recirculation zone, ORZ) extends from the base of the chamber along the lateral wall in all the three cases. Similar results were obtained by Wessman [22] who performed velocity and turbulence measurements using a two-component LDV within a sudden-expansion combustor operating at four different swirl numbers (0, 0.33, 0.58, and 0.99). The swirling flow is generated by eight flat vanes of constant angle (0, 26°, 48°, and 66°). Wessman's data are included also in [17,23]. In the latter, detailed information about the test rig can be found.

The flow fields analysed in [24] are generated by swirlers featuring different angles ($\alpha = 15^\circ, 30^\circ, 45^\circ, \text{ and } 60^\circ$) which correspond to swirl numbers of 0.18, 0.38, 0.67, and 1.16, respectively (values are calculated using Eq. (4), although the chord is not constant along the vane height). The swirler hub, extended about 100 mm upstream from the swirler, exhibits a hemi-spherical nose in order to reduce the flow distortion close to the hub. A five-hole Pitot probe was moved along several radial stations to measure the axial and tangential velocity. Axial velocity profiles show a Gaussian shape only far from the sudden-expansion plane because of the hub wake. A CRZ appears at low swirl number ($S = 0.38$), probably induced by the wake generated by the hub. Instead, the ORZ is barely visible only at the lowest and the highest swirl number.

In [13], particle image velocimetry (PIV) was used to measure mean and fluctuating velocities within an axisymmetric chamber of a water tunnel facility. The flow is swirled upstream of the sudden-expansion plane by means of by eight flat vanes of constant angle (0, 30°, and 45°). Three operating conditions were investigated (S equal to 0, 0.17, and 0.65). The effect of the hub wake on

the axial velocity profiles close to the burner outlet is similar to that observed by Thundil Karuppa [24]. Increase of the swirl number from $S = 0$ to $S = 0.65$ increases both the radial distance of separation between peaks of axial and tangential velocities and the rate of axial velocity decay (a CRZ is visible at $S = 0.65$). The meridian streamlines show a large ORZ and a small recirculation zone close to the chamber corner for the unswirled flow condition. At $S = 0.17$ the corner recirculation zone disappears and the core of the ORZ moves downstream. At high swirl numbers the CRZ causes a reduction of the ORZ, which moves towards the sudden-expansion plane.

These studies allow a comparison of the swirl numbers specified by the authors according to Eq. (2) with swirl numbers calculated using Eq. (3) and (4) (Fig. 2). The values of the swirler design parameters not explicitly declared by the authors were estimated on the basis of test rig schematics provided in the papers.

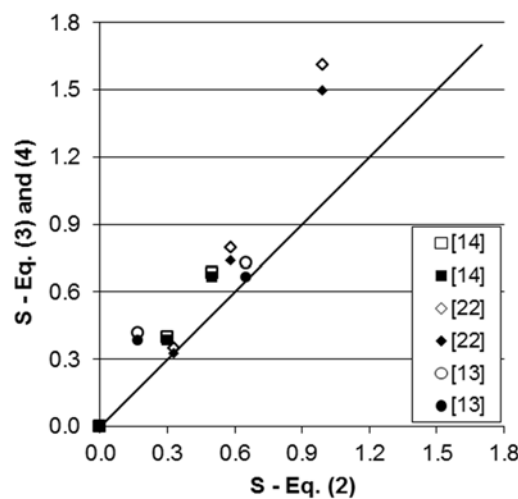


Figure 2 – Comparison of swirl numbers calculated by using Eq. (2) and simplified Eq. (3) and (4). Empty markers: Eq. (3). Solid markers: Eq. (4).

The graph shows that Eq. (3) and (4) overestimate the swirl number value especially at high swirl, as observed also in [13]. At low swirl numbers the overestimation is limited, except for the study of Mak [13]. The best approximation of the swirl number given by Eq. (2) is provided by Eq. (4). Thus, the latter has been used in the following to calculate the swirl number for the experimental data that

do not report the swirl number value.

4. Experimental apparatus and instrumentation

Velocity measurements were acquired by the present authors in the test rig sketched in Fig. 3. The rig, named TAO (Turbogas ad Accesso Ottico – Optical Access Turbogas), is located in the ENEL's experimental area in Livorno (Tuscany, Italy). TAO is an experimental facility for testing industrial size burners at low pressure reacting conditions. It can be operated up to a thermal power of about 800 kW [25–27].

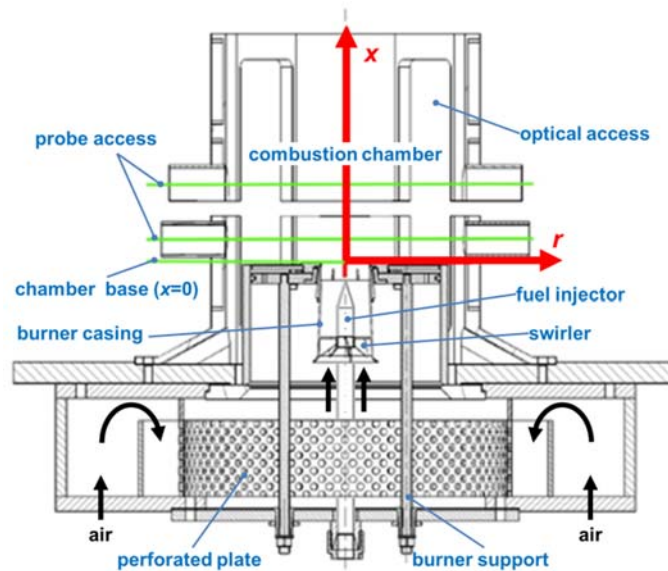


Figure 3 – Schematic of the test rig (TAO). Only the first section of the combustion chamber is shown.

The combustion air, provided by a fan, enters a first plenum located at the bottom of the test rig. From there the air flows throughout a perforated plate and reaches a second plenum which feeds the burner. The flow expands into a vertical chamber before being accelerated by a converging duct placed about 700 mm downstream of the sudden-expansion plane. The converging duct is followed by a dilution section and an exhaust duct. A small tube (not active during the tests presented here) feeds the burner with the fuel. The combustion chamber has a diameter of about 320 mm and features quartz windows to have direct optical access to the flame during reacting tests. Chamber

walls allow also the admission of probes through two lateral access ports.

In the configuration tested, the rig included a premixed burner with an axial swirler comprising eight vanes (Fig. 4). The leading edge of each vane was designed to be aligned to the incoming flow and perpendicular to the centreline of the burner. Vanes progressively curve to reach a trailing angle of 23° so that the swirl number is 0.28 (calculated using Eq. (4)). The swirler is embedded on the burner casing which is a slightly converging duct of minimum diameter $D = 67.6$ mm. The duct shows a small step approximately 20 mm upstream of the exit, which allows a small air-flow inlet for cooling purposes.

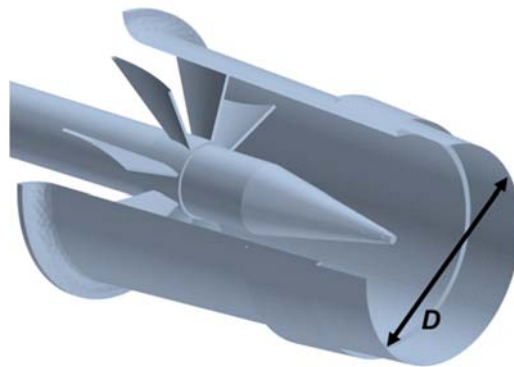


Figure 4 – Model of the burner tested.

Experimental tests were carried out in isothermal conditions at four air mass flow rate, at which the corresponding Reynolds numbers are 162000, 216000, 270000, and 324000, respectively (values are calculated using the mean velocity U_D referred to the burner outlet diameter D). Dimensionless velocity profiles show that the flow field is nearly independent on Reynolds number in all the four operating conditions considered. Data presented in the following sections refer to a Reynolds number of 270000 ($U_D = 62.3$ m/s).

Axial and tangential velocities were measured by using a single hot-wire anemometer. The radial component was verified to be very small and, thus, it was not recorded. Data acquisition was based on a National Instrument system that was able to manage the calibration of the probe and offset the

temperature changes. The calibration was performed each time the probe is positioned on a new plane. Velocities were measured in steady-state conditions along six radii of the combustion chamber located at x/D of 0.53, 0.87, 2.03, 2.37, 6.5, and 6.8. Twenty-one values of each velocity component were acquired along each radius by moving the probe from the combustor axis to a radius of about 100 mm.

5. Results of experimental tests performed on TAO

Figures 5a and 5b plot the radial profiles of the time-averaged axial and tangential velocities, respectively, measured along the radii located at x/D of 0.53, 0.87, 2.03, and 2.37. Note that profiles extend from the combustor axis to approximately two-thirds of the chamber radius (chamber wall is located at about $r/R = 4.7$). Axial velocity profiles were corrected considering the inability of the hot-wire probe used in the experimental tests to determine the sense of the flow direction. In particular, the expected flow reversal outside of the jet was identified by a small cusp along the axial velocity profiles for $r/R > 1$. The same criterion was used in [28] to correct experimental data of radial velocity acquired by using the same measuring technique.

Axial velocity decreases after the expansion in the combustion chamber, but the deceleration is not strong enough to cause a CRZ, as expected (see Fig. 5a). Profiles downstream of $x/D = 0.53$ show a slight double-hump shape, typical of a low-swirling flow. An ORZ sets up far from the combustor axis, as shown by the negative axial velocity values along the first two measuring stations (i.e., $x/D = 0.53$ and 0.87). The two points at which the axial velocity zeroes are joined by the external dashed line labelled q in Fig. 5a. The line, arbitrarily extended to $r/R = 3$, approximately identifies the core of the ORZ. The ORZ axial extension with respect to the chamber step height H (see Fig. 1) results lower than that found by other authors for similar swirl numbers [13, 22]. However, a reliable estimation of the ORZ boundary would require a more detailed characterisation

of the flow field than that performed in the present study, as well as a precise determination of the ORZ core (i.e., points at which axial velocity nullifies).

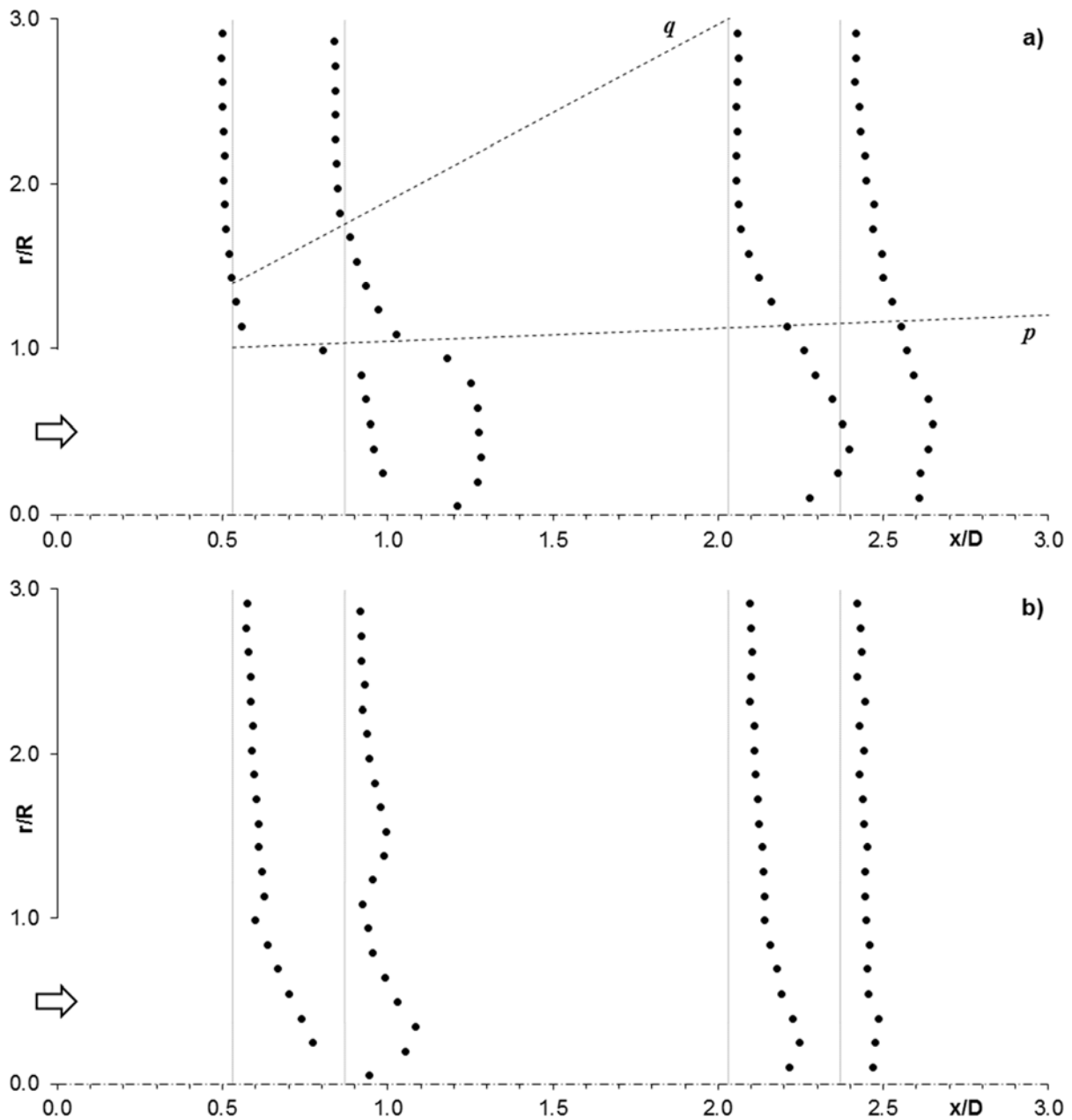


Figure 5 – Radial profiles of axial (a) and tangential velocity (b).

The straight dashed line close to the axis (identified with p in Fig. 5a) indicates the divergence of the jet as a consequence of the sudden expansion. Jet spreading is usually quantified by the half-angle γ , defined as the angle between a line parallel to the centreline and the line joining

the radial locations of the half-maximum axial velocity, $u/u_{max} = 0.5$ [13]. In Fig. 5a, p line joins the radial locations of half-maximum velocity points of profiles $x/D = 0.53$ and 2.03 . The resulting half-angle of jet spreading γ equals about 4.5° , a value lower than that found for expanding flows with similar swirl numbers [12,13]. Note that the angles computed by Mak [13] are calculated using profiles closer to the burner outlet.

The two dashed lines p and q of Fig. 5a allow the identification of three distinct zones: the core region located around the combustor centreline, the outer recirculation zone located across the external dashed line q , and a mixing layer enclosed in between. The radial position of the mixing layer can be identified by looking at the local minima of the tangential velocity profiles (Fig. 5b). These minima occur at around $r/R = 1$ for both the tangential velocity profiles at $x/D = 0.53$ and 0.87 , showing that the mixing layer lies very close the internal dashed line.

As a whole, values plotted in Fig. 5b show a rapid decrease in tangential velocity owing to the tendency of the angular momentum to be conserved. Measurements reveal also a solid-body rotation of the jet core which is still surviving at $x/D = 2.03$. At $x/D = 2.37$ the solid-body rotation is almost decayed and the flow rotates at about the same velocity along the whole radial span.

6. Systematic analysis of the confined low-swirl flow fields

Radial profiles of axial and tangential velocities of each study summarised in the third section of the paper are compared in the following in order to analyse the influence of the combustor design and operating conditions on the flow fields. TAO velocity profiles discussed in the previous section are included in the comparison in order to extend the database. Comparison is carried out with reference to the four measuring stations of TAO (i.e., x/D of 0.53 , 0.87 , 2.03 , and 2.37). Where profile measurement locations in the literature differ from those of TAO, velocities for comparison are obtained by linear interpolation of adjacent data.

All the velocity profiles are made dimensionless by means of the mean axial velocity at the swirler inlet section U_D . For TAO, D refers to the burner outlet since the burner does not feature an upstream duct. Values presented in [14] have been rearranged because they were originally scaled by the inlet centreline velocity ($U_{D,max} = 19.2 \pm 0.4$ m/s). The scaling factor (equal to 1.135) was calculated from the measurements taken in the inlet pipe and provided in the paper. Data acquired by Wessman [22] are extracted from the work by Engdar [23].

Table 1 – Summary of the design/operating parameters of the literature studies considered in the present paper to analyse the confined low-swirling flows. Parameters are referred to designs similar to that of Fig. 1 in which $\beta = 0$.

Ref.	Set Number/Symbol	S	ER	D_r/D	L [mm]	D [mm]	Re
[14]	1 ■	0.3*	1.5	0.19	~100	101.6	110000#
[22]	2 ▲	0.33*	1.94	0.32	~700	50.6	10000
[24]	3 ◆	0.18**	2.34 [§]	0.3	0	107	137000#
[13]	4 □	0.17*	2.5	0.35	~46	40	10000
TAO	5 ●	0.28**	4.7	0.34	~96	67.6	162000÷324000#

*Referred to Eq. (2) – **Calculated using Eq. (4) – [§]Referred to the circular section inscribed – #Calculated at 25°C

Table 1 lists the main design and operating parameters of the literature studies considered in the comparison. TAO values are listed in the last record, as well. Note that sets 1, 2, and 5 refer to designs with nearly the same swirl number (about 0.3), whereas sets 3 and 4 refer to designs featuring a swirl number lower than 0.2. Consequently, two separate comparisons of velocity profiles are performed in the following in order to remove the effect of this parameter and, hence, isolate the effect of other parameters on the flow field. The authors of set 4 do not provide data downstream of $x/D = 1.86$. This latter velocity profile is used in the comparison between set 3 and set 4 at station $x/D = 2.03$.

Figures 6 and 7 show the radial profiles of axial velocity for sets at $S \approx 0.3$ and $S < 0.2$, respectively. In the figures, solid and empty markers refer to high- and low Reynolds-number flows, respectively.

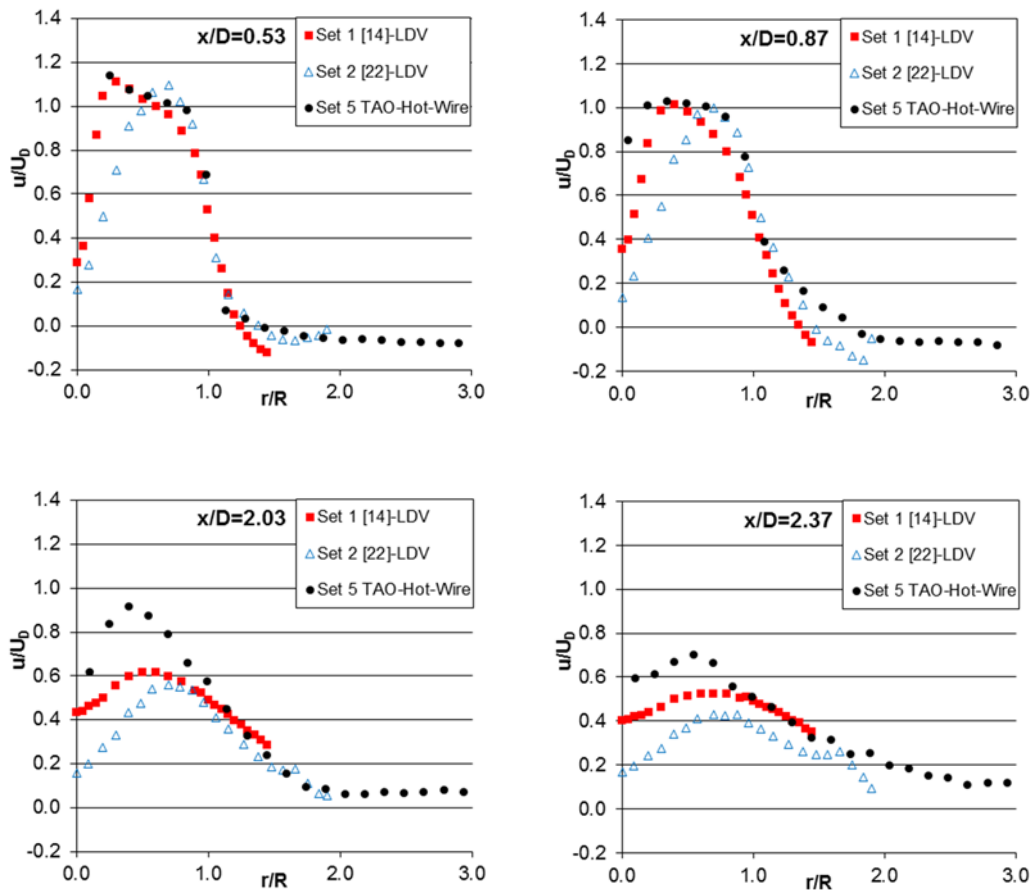


Figure 6 - Radial profiles of axial velocity for swirl number of about 0.3.

Figure 6 states the general agreement of TAO profiles with the axial velocity profiles of the other sets, especially at low velocities. Note in particular the agreement of the radial position at which the axial velocity zeroes for $x/D = 0.53$. Instead, profiles at station $x/D = 0.87$ confirm that TAO ORZ is placed at a dimensionless radial position r/R higher than the ORZs of the other test rigs. In addition, it can be noted that TAO jet core remains closer to the axis if compared with the other data (see, Fig. 6, set 5, $x/D = 0.87$ and downstream stations). This occurrence is probably due to TAO design. In fact, the test rig is the only among those considered in which the swirler is not ducted upstream, the burner casing is slightly converging and the swirler hub shows a slender tail cone at the same time.

The radial position of the velocity peak is clearly affected by the Reynolds number. Sets of data measured at high Reynolds number (i.e., sets 1, 3, and 5) show peaks closer to the axis compared to

sets of data measured at low Reynolds number (i.e., sets 2 and 4). Moreover, considering data plotted in both Fig. 6 and Fig. 7, it appears that the shape of the profiles are mainly influenced by the Reynolds number rather than the swirl number.

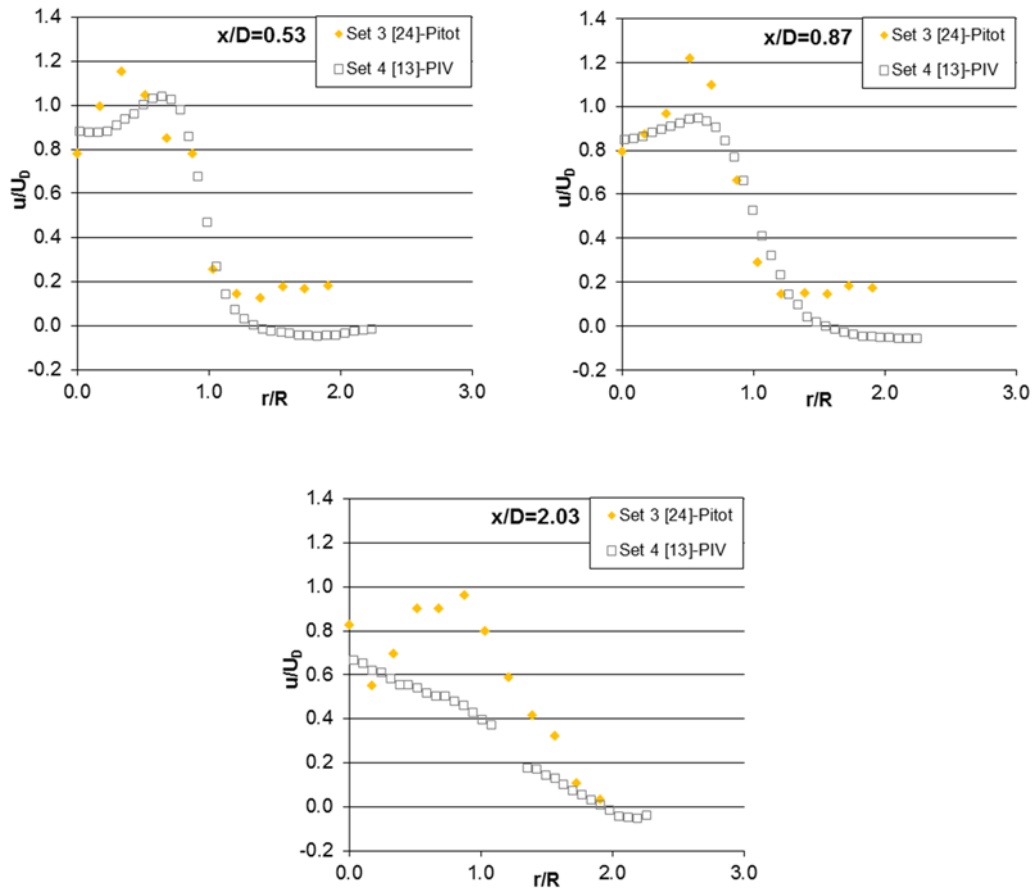


Figure 7 - Radial profiles of axial velocity for swirl number less than 0.2. Note that at $x/D = 2.03$ set 4 is acquired just upstream a sudden expansion. Note also the difficulty of the Pitot probe to measure very low velocities (set 3, values at $r/R > 1.2$).

The D_h/D ratio may also reasonably affect the position of the axial velocity peak because the higher the D_h/D ratio is, the higher is the size of the hub wake. This seems to be confirmed by the comparison of set 1 and set 2 in Fig. 6. However, in the test rig of set 2 the effect of the hub wake is certainly reduced by the long duct (about 700 mm) which connects the swirler to the expansion chamber. Moreover, the distance between the swirler and the chamber constitutes a relevant fraction of the hub diameter D_h in the test rig of set 1, as well. For all these reasons, it is concluded that the

effect of Reynolds number on low-swirl flow fields is by far more relevant than the effect of the hub size for ratios $D_h/D \leq 0.35$. This result is confirmed also by the profiles in Fig. 7, which refer to similar D_h/D ratios. Although in the test rig of set 3 the swirler is placed at the chamber inlet ($L = 0$), the flow field appears to be mainly influenced by the Reynolds number rather than the hub wake.

Profiles plotted in Fig. 6 allow an analysis of the effect of the expansion ratio ER on the velocity field. Spatial evolution of the jet suggests that the lower the ER is, the higher is the axial velocity decay. In particular, all the three velocity profiles (sets 1, 2, and 5 in Fig. 6) roughly overlap at $x/D = 0.53$. Instead, at increased x/D the profile that features the lowest ER (set 1) flattens more rapidly than the other two, while the set 2 velocity ($ER = 1.94$) decays faster than that of set 5 ($ER = 4.7$). Moreover, from $x/D = 0.87$ profiles of Fig. 6, it appears also that the zero axial velocity point moves towards the chamber wall as the ER increases. Thus, ER affects also the ORZ in: i) location, from which it can be concluded that the further from the axis, the higher ER design; ii) recirculation velocity, which tends to be higher for lower ER .

Radial profiles of tangential velocity are plotted in Fig. 8. Values of set 3 are included as well, although the test rig operates with a swirl number lower than 0.2. This is because tangential velocities are not available for set 4, and thus a comparison is not possible.

Sets 1, 2, and 5 show approximately the same radial position of the mixing layer (see the local minima at about $r/R = 1$), whereas set 3 does not allow a precise location of the mixing layer because of the poor spatial resolution of the data (the local minimum at about $r/R = 0.5$ is due to a small mixing layer generated downstream of the hub wake).

Tangential velocity profiles confirm the effect of the Reynolds number on the flow field already observed in axial velocity profiles. In fact, looking at sets having similar swirl number (i.e., sets 1, 2, and 5), it can be seen that the velocity peak is closer to the axis for sets at higher Reynolds number (1 and 5). In contrast, the effect of D_h/D on tangential velocities is almost negligible.

Increase the distance L contributes to a slight reduction of the gradients in the profiles because of tangential momentum conservation. For instance, set 2 shows a quite low peak magnitude close to the axis, although the swirl number of the flow is the highest among the sets considered.

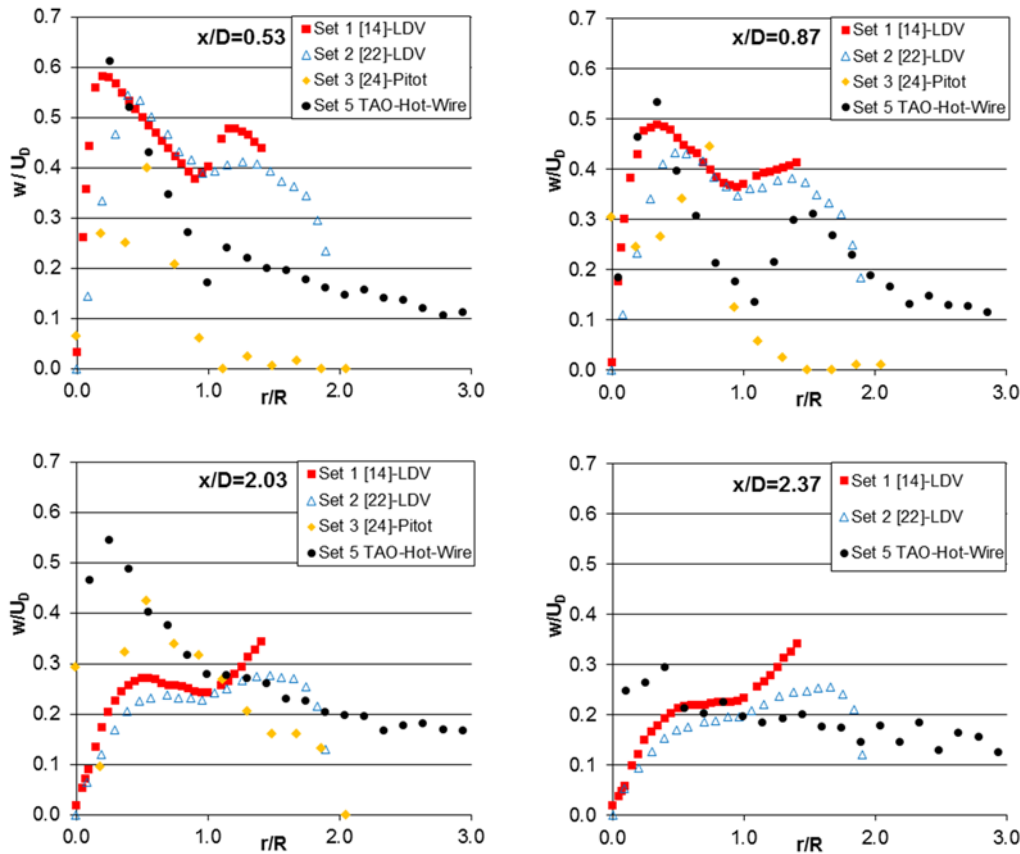


Figure 8 - Radial profiles of tangential velocity for swirl number of about 0.3. Set 3 ($S = 0.18$) is included as well.

Bearing in mind the effect of Re , D_h/D , and L on the tangential velocity field, the influence of expansion ratio (ER) is clearly visible in Fig. 8: a lower ER leads to a higher tangential velocity decay of the jet core (comparing sets 1 and 2 with sets 3 and 5). In addition, in the test rigs featuring a small ER (sets 1 and 2), the tangential velocity of the jet core stream decays faster than the velocity of the outer stream flowing next to the mixing layer. This results in tangential profiles which increase with r/R at $x/D = 2.03$ and 2.37 and feature slopes that increase as ER decreases.

7. Conclusions

Mean axial and tangential velocities acquired within five test rigs are compared in order to analyse the flow field resulting from a sudden expansion of low-swirling flows into confined chambers. The test rigs reproduce the design of small laboratory combustors in which the swirl motion is generated by vaned axial swirlers.

The database of four sets of measurements found in the literature is extended with a fifth set of experimental values that the present authors acquired by using a hot-wire probe. Experimental tests were performed at high Reynolds number on a laboratory combustor featuring an expansion ratio much higher than that usually adopted in similar facilities. Thus, the new set of data represent an original contribution to the sets already published in the literature.

Mean velocity profiles are compared at swirl numbers as similar as possible in order to remove the effect of this parameter and focus the attention on other parameters less investigated in the literature such as the expansion ratio (ER), the ratio between the hub diameter and the swirler diameter (D_h/D), the axial distance between the swirler and expansion plane (L), and the Reynolds number of the swirling flow.

The comparison of the five sets of measurements show that:

- The flow field of low-swirl combustors is mostly affected by the Reynolds number. In particular, velocity peaks are less displaced from the combustor axis when the test rigs operate at high Reynolds numbers.
- Expansion ratio is the most relevant design parameter among those considered. Lower ER s cause a higher axial decay of both axial and tangential velocities of the core of the jet. Moreover, for low ER s, the tangential velocity decay of the stream outside of the jet is more limited than the velocity decay of jet core. Lower values of ER lead also to ORZ closer to the jet and higher velocities within the ORZ.

- The effect of the swirler hub is rather limited far from the expansion plane and is negligible compared to the effect of Reynolds number.
- Increase the axial distance L smooths the gradients in tangential velocity profiles before the flow enters into the chamber.

Acknowledgements

Authors gratefully acknowledge the ENEL staff of the experimental area of Livorno and Regione Veneto that partially funded the research activities.

References

- [1] J.M. Beer, N.A. Chigier, Combustion aerodynamics, Robert E. Krieger Publishing Company Inc., Malabar, Florida, USA, 1983.
- [2] K. Oberleithner, C.O. Paschereit, R. Seele, I. Wygnanski, Formation of turbulent vortex breakdown: intermittency, criticality and global instability, *AIAA J.* 50 (2012) 1437–1452.
- [3] R. Cheng, H. Levinsky, Lean premixed burners, in: D. Dunn-Rankin, Lean combustion: technology and control, Academic Press, London, 2007, pp. 161–177.
- [4] N. Syred, J.M. Beer, Combustion in swirling flows: a review, *Combust. Flame* 23 (1974) 143–201.
- [5] N. Syred, 40 Years with swirl, vortex, cyclonic flows, and combustion, 49th AIAA Aerospace Sciences Meeting including the New Horizons Forum and Aerospace Exposition (2011), paper AIAA2011-105.
- [6] D.G. Lilley, Swirl flows in combustion: a review, *AIAA J.* 15 (1977) 1063–1078.
- [7] O. Lucca-Negro, T. O’Doherty, Vortex breakdown: a review, *Prog. Energy Combust. Sci.* 27 (2001) 431–481.
- [8] M.R. Johnson, D. Littlejohn, W.A. Nazeer, K.O. Smith, R.K. Cheng, A comparison of the flowfields and emissions of high-swirl injectors and low-swirl injectors for lean premixed gas turbines, *Proc. Combust. I.* 30 (2005) 2867–2874.
- [9] T.M. Farag, M. Shimizu, M. Arai, H. Hiroyasu, Flow measurement in a swirl combustor in two cases of with and without combustion, *Bull. JSME* 27 (1984) 521–528.

- [10] S. Mondal, A. Dattab, A. Sarkar, Influence of side wall expansion angle and swirl generator on flow pattern in a model combustor calculated with $k-\epsilon$ model, *Int. J. Therm. Sci.* 43 (2004) 901–914.
- [11] P.J. Foster, J.M. Macinnes, F. Schubnell, Isothermal modelling of a combustion system with swirl: a computational study, *Combust. Sci. Technol.* 155 (2000) 51–74.
- [12] N.A. Chigier, A. Chervinsky, Experimental investigation of swirling vortex motion in jets, *J. Appl. Mech.* 34 (1967) 443–451.
- [13] H. Mak, S. Balabani, Near field characteristics of swirling flow past a sudden expansion, *Chem. Eng. Sci.* 62 (2007) 6726–6746.
- [14] S.C. Favaloro, A.S. Nejad, S.A. Ahmed, Experimental and computational investigation of isothermal swirling flow in an axisymmetric dump combustor, *J. Propul.* 7 (1991) 348–356.
- [15] D.L. Rhode, D.G. Lilley, D.K. McLaughlin, Mean flowfields in axisymmetric combustor geometries with swirl, 20th AIAA Aerospace Sciences Meeting (1982), paper 82-0177.
- [16] S.A. Ahmed, A.S. Nejad, Swirl effect on confined flows in axisymmetric geometries, *J. Propul. Power* 8 (1992) 339–345.
- [17] P. Wang, X.S. Bai, M. Wessman, J. Klingmann, Large eddy simulation and experimental studies of a confined turbulent swirling flow, *Phys. Fluids* 16 (2004) 3306–3324.
- [18] A.H. Lefebvre, *Gas turbine combustion*, Taylor & Francis Group, Boca Raton, Florida, USA, 2010.
- [19] S.A. Beltagui, N.R.L. Maccallum, The modeling of vane-swirled flames in furnaces, *J. I. Fuel* 49 (1976) 193–200.
- [20] W.L.H. Hallett, D.J. Toews, The effect of inlet conditions and expansion ratio on the onset of flow reversal in swirling flow in a sudden expansion, *Exp. Fluids* 5 (1987) 129–133.
- [21] P.A. Dellenback, D.E. Metzger, G.P. Neitzel, Measurement in turbulent swirling flow through an abrupt axisymmetric expansion, *AIAA J.* 26 (1988) 669–681.
- [22] M. Wessman, J. Klingmann, B. Noren, Experimental studies of confined turbulent swirling flows, 7th International Symposium on Applications of Laser-Doppler Anemometry to Fluid Mechanics (1994), paper 19.3.
- [23] U. Engdar, J. Klingmann, Investigation of two-equation turbulence models applied to a confined axis-symmetric swirling flow, *ASME Comp. Technol.* 448 (2002) PVP2002-1590.
- [24] R. Thundil Karuppa, V. Ganesan, Study on the effect of various parameters on flow development behind vane swirlers, *Int. J. Therm. Sci.* 47 (2008) 1204–1225.

- [25] S. Tiribuzi, CFD modelling of thermoacoustic oscillations inside an atmospheric test rig generated by a DLN burner, ASME Turbo Expo 2004, paper GT2004-53738.
- [26] I. Brunetti, G. Riccio, N. Rossi, A. Cappelletti, L. Bonelli, A. Marini, E. Paganini, F. Martelli, Experimental and numerical characterization of lean hydrogen combustion in a premix burner prototype, ASME Turbo Expo 2011, paper GT2011- 45623.
- [27] M. Cerutti, S. Cocchi, R. Modi, S. Sigali, G. Bruti, Hydrogen fueled dry low NO_x gas turbine combustor conceptual design, ASME Turbo Expo 2014, paper GT2014-26136.
- [28] D.G. Lilley, Investigations of flowfields found in typical combustor geometries, Report No. 3869, Appendix C, NASA Lewis Research Center, Cleveland, Ohio, USA, 1985.